ELSEVIER

Coordination Chemistry Reviews
174 (1998) 255–282

COORDINATION CHEMISTRY REVIEWS

Hydrogen bonding in tungsten(VI) salicylate free acids[1]

Timothy E. Baroni [a], Scott Bembenek [a], Joseph A. Heppert [a,*], Rolande R. Hodel [a], Brian B. Laird [a], Martha D. Morton [a], Denise L. Barnes [a], Fusao Takusagawa [b]

[a] *Department of Chemistry, the University of Kansas, Lawrence, KS 66045, USA*
[b] *Molecular Structure Laboratory, the University of Kansas, Lawrence, KS 66045, USA*

Received 21 August 1997; accepted 27 January 1998

Contents

* Corresponding author.

[1]Dedicated to Professor Daryle Busch on the occasion of his 70th birthday.

PII S0010-8545(98)00055-1

Abstract

Hydrogen-bonded free acid dimers of the formula $[W(X)Cl_3(Hsal\text{–}R)]_2$ (where X = O (**1**), NC_6H_3-2,6-Me_2 (**2**), Ph_2C_2 and Hsal–R = substituted salicylate monoanion) are prepared through reactions between $W(X)Cl_4$ precursors and functionalized salicylic acids ($H_2sal\text{–}R$).

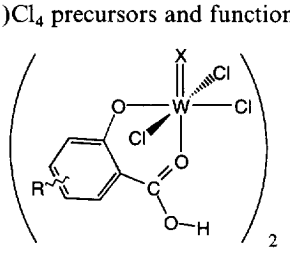

I

The free acids are stable at ambient temperature and exist as dimers in solution, although the structure of the dimer is not known. Spectroscopic studies show that the electronic characteristics of the π-donor ligands directly affect the electronic environments of the carboxylate functionality. This influence is observed in weaker binding constants of diethyl ether (K_X) as the X ligand becomes more strongly π donating: $O \geqslant NC_6H_3\text{–}2,6\text{-}Me_2 > Ph_2C_2$. In other words, the oxo and aryl imido species are more acidic than the diphenylacetylene compounds in the Brønsted sense owing to the higher Lewis acidity of their tungsten centers. Salicylate adducts of the type $W(=X)Cl_3(Hsal\text{–}R)\cdots OR'_2$ (X = O (**3**), $NC_6H_3\text{–}2,6\text{-}Me_2$ (**4**)) and $W(=X)Cl_3(Hsal\text{–}R)\cdots NEt_3$ (X = O (**5**), $NC_6H_3\text{–}2,6\text{-}Me_2$ (**6**)) have been isolated and characterized. A comparison of two structures, $W(=NC_6H_3\text{–}2,6\text{-}Me_2)Cl_3(Hsal\text{–}3\text{-}Me\cdots L)$ where $L = OEt_2$ (**4c**) and NEt_3 (**6c**), shows that **6c** has more charge localization on both the carboxylate group and tungsten center than **4c**. The charge separation in amine adducts (i.e. salts) contributes to association of these salts with the free acid (i.e. $W(X)Cl_3(Hsal\text{–}R\cdots L)\cdots[W(X)Cl_3(Hsal\text{–}R)]$). The strong hydrogen bonding exhibited by the free acids leads to the formation of supramolecular complexes organized around poly(ether) templates, including dimethoxyethane (in **3e**) and 18-crown-6.

Keywords: Tungsten, phenoxides, salicylates, hydrogen bonding, binding constants, supramolecular.

1. Introduction

Hydrogen bonding in Brønsted acid transition metal complexes is a subject of significant research interest [1–15]. Hydrogen bonding lends new dimensions to intermolecular interaction to beyond simple shape recognition, making compounds containing such functionality crucial components in biomimetic complexes [1–6], molecular receptors [7–11], magnetic assemblies and optical materials [12–15]. These targets and the feasibility of a stepwise approach to the preparation of complex hydrogen-bonded solid-state materials account for the interest in studying transition metal complexes with hydrogen bonding functionality [12–15].

Our studies of tungsten compounds with hydrogen bonding functional groups began with the inadvertent isolation of chelating phenol–phenolate and salicylate complexes of tungsten oxo and aryl imido precursors [16,17]. These compounds are related to a number of previously known phenol–phenolate and salicylate complexes [18–21]. Over the last several years, various investigators have identified additional examples of both classes of compounds [22–24]. Studies of the hydrogen bond affinity of these complexes indicated that the conformation of the phenol–phenolate chelate had a strong influence on association constants with Lewis bases [16]. The hydrogen bonding characteristics of complexes vary as the chelate's electronic character changes. This electronic behavior can range from alkoxide to phenol-like character. Therefore, it is possible to control systematically the hydrogen bond strength of these Brønsted acids through (1) modifications of the electronic structure and topology of the chelating ligands, and (2) changes in the Lewis acidity of the tungsten fragment. A variety of tunable Brønsted acid complexes would allow us to vary the physical characteristics of the molecules in specified media, modify the binding affinity of a range of organic Brønsted bases at receptor sites containing these complexes, and regulate the modes by which these complexes undergo self-assembly into hydrogen-bonded multidimensional arrays.

The objective of this study was to prepare an assortment of salicylate-substituted tungsten complexes amenable to studies of hydrogen bonding in non-aqueous media. A more specific goal was to understand how the hydrogen bonding behavior of Hsal free acid complexes are influenced by (1) the substituents on the relatively conformationally rigid salicylate (Hsal–R) ligand and (2) the tungsten center. We report the synthesis of a family of free acids, $W(X)Cl_3$(Hsal–R) (X=O, NC_6H_3–2,6-Me_2, Ph_2C_2, and R=H, Me, Ph, Cl and OH), along with their ether and amine adducts. NMR titrations with ether and triethylamine were performed to gauge the strength of these adduct hydrogen bond interactions. X-ray structural studies of **3e** and the structurally analogous pair of **4c** and **6c** have been performed to further the interpretation of these studies.

2. Results and discussion

2.1. Synthesis and characterization of salicylate complexes

The preparation of parent free acid complexes of formula $W(X)Cl_3$(Hsal–R) (X=O, NC_6H_3–2,6-Me_2, Ph_2C_2) is achieved by combining the $W(X)Cl_4$ precursor

[25,26] with a substituted salicylic acid (H_2sal–R) in dichloromethane (Eq. (1)). For the oxo and 2,6-dimethylaryl imido systems, the free acids precipitate spontaneously from solution without heating as red–purple or metallic gray analytically pure microcrystalline powders respectively. The resulting free acids are insoluble in hydrocarbon solvents, having greater solubility in polar media such as chloroform.

$$W(X)Cl_4 + H_2sal\text{–}R \rightarrow \tfrac{1}{2}[W(X)Cl_3(Hsal\text{–}R)]_2 \quad (1)$$

Solution molecular weight studies indicate that all of the oxo and aryl imido complexes are dinuclear in benzene solution, within tolerances for experimental error (±5%) [27]. Although the free acids are isolated as crystalline materials, only one example of the tungsten diphenylacetylene free-acid complex has been structurally characterized [17].

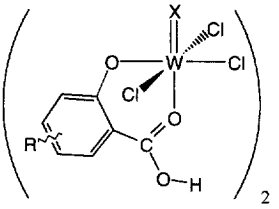

I

The structure of **I** is in sharp contrast to the eight-membered cyclic arrangement for classic hydrogen-bonded acid dimers because there are no groups hydrogen bonded to the acidic proton. This observation can be attributed to a combination of increased steric congestion and decreased Brønsted basicity at the carbonyl moiety of the acid. As chloride is the most accessible Brønsted base present, O–H···Cl interactions seem to be the most likely mode of association in solution [28–30] (for similar hydrogen bond interactions involving N–H···Cl bonds see Ref. [31]). The molecule $W(Ph_2C_2)Cl_3$(Hsal–3-Me) exhibits a solution molecular weight 20% below the expected dinuclear value, indicating that a significant fraction of monomer is present in benzene solution. The methyl substituent on the salicylate ligand and the formal d^2 electron count of the tungsten acetylene unit make the carboxylic acid group of this complex the most electron rich among the three classes of complexes studied. It is probable that the increased electron density at the carboxylate results in reduced hydrogen bond strength and a measurable population of monomer according to the equilibrium expressed in Eq. (2). Tungsten phenol–phenoxide complexes of formula $W(X)Cl_3(OArOH\cdots OEt_2)$ display a similar correlation between the electron density of the hydroxyl group and the binding constant of ether [16]. For $W(X)Cl_3$(Hsal) compounds, efforts to monitor directly the monomer–dimer equilibria as a function of the R substituent by NMR dilution experiments were largely inconclusive because acceptable ^{1}H NMR spectra of all the free acids are only obtained near the maximum solubility of the complexes.

$$[W(X)Cl_3(Hsal\text{–}R)]_2 \rightleftarrows 2W(X)Cl_3(Hsal\text{–}R) \quad (2)$$

^{13}C NMR spectroscopy provides more direct information about the electronic environment of the carbonyl unit in the free acids. As is observed for simple benzoic acids, the ^{13}C chemical shift of the carboxylate carbon atoms on the salicylate ring correlate with Hammett σ parameters in the oxo, aryl imido and diphenylacetylene complexes [32–34]. Although these trends are not derived from reaction rates, they are still indicative of the capacity of the oxo-, aryl-imido- and diphenylacetylene-substituted tungsten centers to stabilize developing negative charge at the carboxylate group. Both the oxo and aryl imido groups are strong π-donor ligands that are bound to formally d^0 tungsten centers. These similarities result in a relatively small difference in the ρ values of the two series. The Hammett correlation for the $W(Ph_2C_2)Cl_3$(Hsal–R) complexes has a larger negative slope, indicating that the tungsten η^2-diphenylacetylene unit is less able to stabilize the development of negative charge at the carboxylate group. This observation seems consistent with the formal d^2 electron configuration at tungsten. We would reach the same conclusion about the relative ability of the X ligands to assist in the stabilization of negative charge at the carbonyl group if the acetylene ligand were considered to be a *cis*-stilbene dianion, $[Ph_2C_2]^{2-}$. The anticipated ordering of π-donor ligand strength is $O^{2-} \leqslant NAr^{2-} \ll Ph_2C_2^{2-}$. The principal chemical consequence of this trend is that acetylene complexes form observably weaker hydrogen bonds than either their oxo or aryl imido analogs, as has already been exhibited through the partial dissociation of the $W(Ph_2C_2)Cl_3$(Hsal–3-Me) dimer in benzene solution.

$$[W(X)Cl_3(Hsal\text{–}R)]_2 + 2Et_2O \rightleftarrows 2W(X)Cl_3(Hsal\text{–}R\cdots OEt_2) \quad (3)$$

Diethyl ether adducts of these acids can be isolated either by dissolving the free acids in diethyl ether or through direct reaction between the $W(X)Cl_4$ precursor and H_2sal–R in neat ether (Eq. (3)). Unlike the phenol–phenoxide complexes noted above, ether adducts of the free acids cannot be isolated from dilute hydrocarbon solutions of ether [16,18–20]. Such solutions habitually yield crystalline $[W(X)Cl_3(Hsal\text{–}R)]_2$. Moreover, ether is easily removed from $W(X)Cl_3(Hsal\text{–}R\cdots OEt_2)$ complexes by dissolution in hydrocarbon solvents or through exposure to vacuum. This complicates the isolation of stoichiometric ether adducts, as the ether is only weakly bound to the acidic proton (*vide infra*). Although formation of the ether adducts is likely to be enthalpically favored [35], the dissociation of ether should be somewhat entropically unfavorable. The entropic contribution, combined with the high vapor pressure of diethyl ether, disfavors the isolation of ether adducts from non-coordinating solvents. This behavior can be circumvented by using less volatile ethers, such as dimethoxyethane or 18-crown-6. Crystals of $[W(=O)Cl_3(Hsal)]_2\cdots$(dme) and $[W(=X)Cl_3(Hsal)]_4\cdots$(18-crown-6) (X=O, NC_6H_3–2,6-Me_2, or Ph_2C_2) are isolated from dichloromethane or toluene solutions.

Tetrahydrofuran plays a different role in the chemistry of the Hsal complexes. The THF adducts, $W(X)Cl_3(Hsal\text{–}R\cdots THF)$, can be observed spectroscopically through the treatment of the free acid species with THF, but these adducts rapidly decompose to generate simple salicylate complexes of formula $W(X)Cl_2$(sal–R)(THF) (**9b** and **10b**). This is not solely due the increased Brønsted

basicity of THF. Secondary and tertiary amine adducts of the tungsten salicylates are quite stable (*vide infra*). We hypothesize that, as THF abstracts a proton from the carboxylic acid, it undergoes proton-induced ring opening (Scheme 1). This provides a pathway for the irreversible deprotonation of the complex, with the result that the remaining $[W(X)Cl_3(sal)]^-$ moiety is prone to the elimination of chloride. THF has been observed to induce a similar hydrogen chloride elimination from tungsten phenol–phenoxide complexes [17–20].

$$[W(X)Cl_3(Hsal\text{–}R)]_2 + 2NR_3 \rightarrow 2W(X)Cl_3(Hsal\text{–}R\cdots NR_3) \quad (4)$$

Tertiary and secondary amines react with the free acids to generate hydrogen-bonded adducts (i.e. alkylammonium salts), $W(=X)Cl_3(Hsal\text{–}R\cdots NEt_3)$ and $W(=X)Cl_3(Hsal\text{–}R\cdots NEt_2H)$ (Eq. (4)). The spectroscopic characteristics of the amine products resemble those of the etherates. Chemical shifts of the trialkylammonium protons characteristically appear downfield of the carboxylic acid protons observed for the free acids and etherate adducts. These salts are soluble in common aromatic solvents, dichloromethane, and chloroform.

Difunctional free acids, based on covalently linked salicylate and phenylene imido bridging units, can be prepared through direct reactions with the metal precursors (**II** and **III**). These acids are virtually insoluble in non-polar solvents, but are sparingly soluble in coordinating solvents like diethyl ether. Reactions between the difunctional acids (such as **8b**) and di- and poly-functional hydrogen bond acceptors,

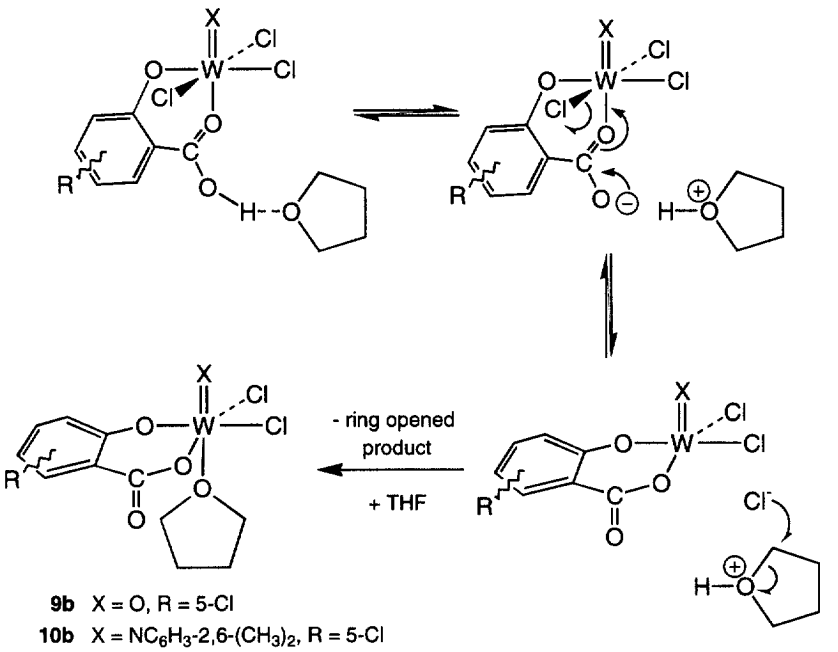

Scheme 1. Irreversible depronation of salicylate by ring-opening of THF.

such as dimethoxyethane, 18-crown-6, and tetramethylethylenediamine (tmeda), produce insoluble powders that are difficult to purify.

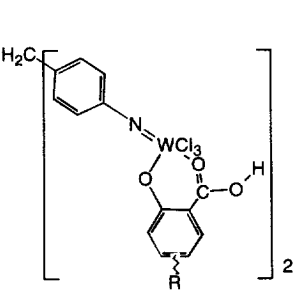

II

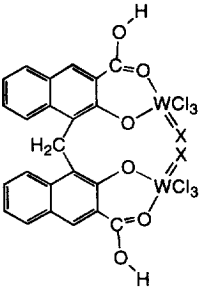

III

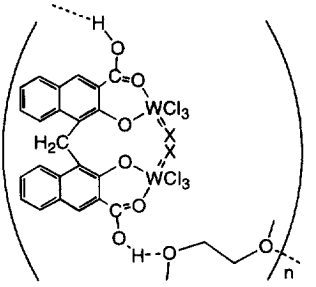

IV

We assume that the poor solubility of both the difunctional free acids and their adducts with polyfunctional hydrogen bond acceptors results from the formation of extended hydrogen bonding networks (**IV**).

2.2. *Structures of the hydrogen-bonded complexes*

$[W(=O)Cl_3(Hsal)]_2\cdots(dme)$ (**3e**), shown in Fig. 1, exemplifies the structural characteristics of Brønsted base adducts of the free acid complexes. Pertinent bond distances and angles for **3e** are found in Tables 1 and 2 respectively. The W=O bonds are characteristically short, being 1.68(1) Å for W(1) and 1.684(9) Å for W(2). This distance is strikingly shorter than those observed in tungsten–oxo complexes bearing an alkoxide or π-donor aryloxide ligand [16,18–20,22–24]. An average phenolate W–O distance of 1.88(1) Å is observed for the salicylate ligands. This is indicative of the weak π-donation usually observed for phenoxide ligands and distinguishes them from the short 1.79(1) Å W–O distances observed for chelating bis-phenoxide ligands engaged in π-donation [16,18–20]. Based on the acidity of the carboxylate unit, the complex might be expected to adopt an η^1-carboxylate anion structure, instead of the observed η^1-phenoxide coordination mode [22–24].

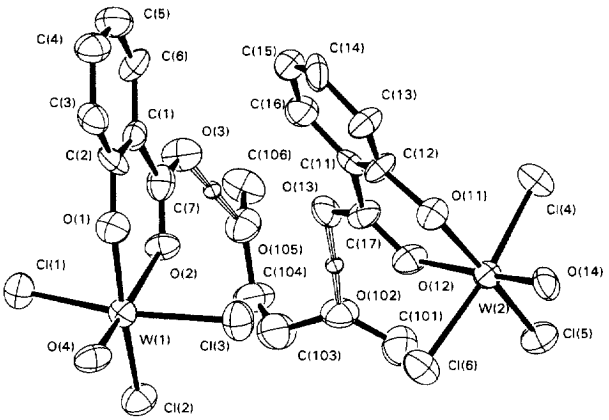

Fig. 1. An ORTEP diagram of the molecular structure of $[W(=O)Cl_3(Hsal)]_2\cdots(dme)$ (**3e**). Hydrogen atoms other than those involved in hydrogen bonds are omitted for clarity.

Table 1
Intramolecular bond distances for $[W(=O)Cl_3(Hsal)]_2\cdots(dme)$ (**3e**). Estimated standard deviations in the least significant figure are given in parentheses

Atoms		Distance (Å)	Atoms		Distance (Å)
W(1)	Cl(1)	2.341(4)	W(2)	Cl(4)	2.334(4)
W(1)	Cl(2)	2.3113(4)	W(2)	Cl(5)	2.310(4)
W(1)	Cl(3)	2.324(4)	W(2)	Cl(6)	2.308(4)
W(1)	O(1)	1.89(1)	W(2)	O(11)	1.87(1)
W(1)	O(2)	2.224(9)	W(2)	O(12)	2.20(2)
W(1)	O(4)	1.68(1)	W(2)	O(14)	1.684(9)
O(2)	C(7)	1.26(2)	O(12)	C(17)	1.25(2)
O(3)	C(7)	1.27(2)	O(13)	C(17)	1.27(2)
O(3)	H(01)	1.285[a]	O(13)	H(02)	1.306[a]

[a] H(01) and H(02) were not found in the Fourier difference map, but were arbitrarily placed halfway between their respective acid oxygen atoms, O(3) and O(13), and their ether oxygen atoms, O(105) and O(102).

Several factors may account for the counterintuitive structure. First, the hydrogen-bond-induced dimerization of $W(X)Cl_3(Hsal)$ complexes, a process not observed for $W(X)Cl_3(Hcat)$ complexes, may add to the thermodynamic stability of the η^1-phenoxide structure. Second, the pK_a of a phenol group is probably decreased less on coordination to tungsten than the pK_a of a similarly coordinated carboxylic acid unit. Finally, the phenoxide ligand forms a stronger W–O σ-bond than does a resonance-stabilized η^1-carboxylate anion.

The ligands cis to the oxo unit have an average of 8° deviation from an idealized octahedral geometry away from the oxo ligand. This characteristic of the strong trans influence of the oxo group may be accentuated by the relatively small steric demand of the coordinated carbonyl unit [16–24]. Surprisingly, the phenoxide shows

Table 2
Intramolecular bond angles for $[W(=O)Cl_3(Hsal)]_2\cdots(dme)$ (**3e**). Estimated standard deviations in the least significant figure are given in parentheses

Atoms			Angle (deg)	Atoms			Angle (deg)
Cl(1)	W(1)	Cl(2)	86.4(1)	O(1)	W(1)	O(4)	95.7(4)
Cl(1)	W(1)	Cl(3)	163.7(1)	O(2)	W(1)	O(4)	175.9(4)
Cl(1)	W(1)	O(1)	88.2(3)	W(1)	O(1)	C(2)	140.8(9)
Cl(1)	W(1)	O(2)	81.7(3)	W(1)	O(2)	C(7)	131.1(9)
Cl(1)	W(1)	O(4)	98.9(4)	O(1)	C(2)	O(3)	117(1)
Cl(2)	W(1)	Cl(3)	88.6(1)	Cl(4)	W(2)	Cl(5)	86.2(1)
Cl(2)	W(1)	O(1)	164.4(3)	Cl(4)	W(2)	Cl(6)	165.0(1)
Cl(2)	W(1)	O(2)	84.6(3)	Cl(4)	W(2)	O(11)	86.5(3)
Cl(2)	W(1)	O(4)	99.6(4)	Cl(4)	W(2)	O(12)	82.1(3)
Cl(3)	W(1)	O(1)	92.5(3)	O(11)	W(2)	O(14)	95.9(4)
Cl(3)	W(1)	O(2)	82.3(3)	O(12)	W(2)	O(14)	177.1(4)
Cl(3)	W(1)	O(4)	97.3(4)	W(2)	O(11)	C(12)	137.8(9)
O(1)	W(1)	O(2)	80.2(4)	W(2)	O(12)	C(17)	131.7(9)
Cl(5)	W(2)	O(14)	99.9(4)	Cl(4)	W(2)	O(14)	97.7(3)
Cl(6)	W(2)	O(11)	93.5(3)	Cl(5)	W(2)	Cl(6)	89.8(2)
Cl(6)	W(2)	O(12)	83.0(3)	Cl(5)	W(2)	O(11)	163.3(3)
Cl(6)	W(2)	O(14)	97.3(4)	Cl(5)	W(2)	O(12)	82.9(3)
O(11)	W(2)	O(12)	81.2(4)	O(13)	C(17)	C(11)	116(1)

the smallest deviation of the cis ligands (5.7°) from an idealized octahedron; the opposite of this trend is observed in related complexes that contain strongly π-donating phenoxides. Differences between the bond distances and angles of the monoanionic salicylate chelate and corresponding catecholate monoanions are relatively minor [18–20]. The salicylate W–O–C_{Ar} angle is 5° larger (average) than the Hcat complex to accommodate the expanded six-membered chelate and the long W–$O_{carbonyl}$ distance of 2.29(1) Å. As has been observed with other η^1-carboxylate ligands, the presence of the hydrogen bond confirms that the hydroxyl group of the carboxylate is not bound to the metal center [18–20,22–24]. By bonding to the non-ligated oxygen, the proton associates with the more basic oxygen of the carboxylate, and has greater accessibility for intermolecular hydrogen bonding. The average observed O–H···O distance of 2.56(4) Å is characteristic of strong hydrogen bonds in these systems.

The intermolecular packing of the **3e** molecules in the solid state is rooted in the unusual dihedral relationship between the two salicylate complexes bound to dimethoxyethane. The two subunits are oriented by aryl group π-interactions with a centroid–centroid distance between the rings of 4.48 Å [36,37]. The distance from C(15) to the centroid of the salicylate on W(1) (hereafter abbreviated cent[sal(1)]) of 3.59 Å suggests a C–H···π interaction with the adjacent salicylate complex [36,37]. The interplanar angle θ created by the rings is 50.5°, showing an appropriate orientation for this type of interaction [38,39]. It is noteworthy is that **3e** has θ values slightly lower than those referenced for edge-to-face interactions [38,39] and its centroid–centroid distance is slightly shorter. With a smaller θ, the aryl rings

should interact more strongly owing to decreased steric repulsions, thus shortening the centroid–centroid distance. This suggests a continuum of bond angles and distances for π-aryl interactions that lie between the two extremes of π-stacking ($\theta < 30°$, ~3 to 4 Å) and edge-to-face interactions ($30 < \theta < 90°$, ~4 to 6 Å) [36,37].

One of the methyl carbon atoms of dimethoxyethane, C(101), is 3.63 Å away from cent[sal(1)]. This resulting C–H···π interaction gives the crystal an inherently higher degree of order—effectively controlling the assembly of the crystal in the direction of the *ab*-plane of the lattice. A methylene carbon of dimethoxyethane, C(104), participates in the same type of interaction with cent[sal(2)] at a distance of 3.95 Å [40,41]. This association repeats along the *ac*-plane of the crystal, promoting its assembly through these intermolecular stacking interactions. These two C–H···π interactions lend an infinite chain structure to the crystal lattice, showing how non-covalent interactions can be used to promote self-assembly.

The complexes **4c** and **6c** (in Fig. 2) illustrate the structural differences of the same basic metallic unit as one bond increases in ionic character. Pertinent bond

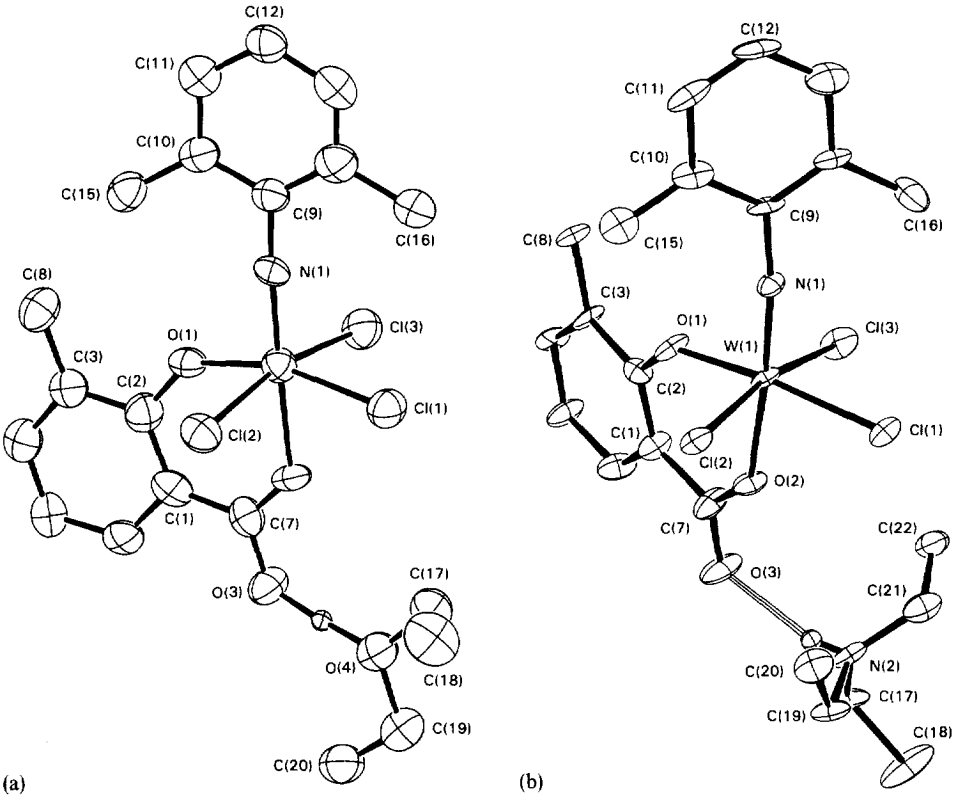

Fig. 2. ORTEP diagrams of the molecular structures of (a) $W(=NC_6H_3\text{-}2,6\text{-}Me_2)Cl_3(Hsal\text{-}3\text{-}Me\cdots OEt_2)$ (**4c**) and (b) $W(=NC_6H_3\text{-}2,6\text{-}Me_2)Cl_3(Hsal\text{-}3\text{-}Me\cdots NEt_3)$ (**6c**). Hydrogen atoms other than those involved in hydrogen bonds are omitted for clarity.

distances and angles for **4c** are given in Tables 3 and 4 and for **6c** in Tables 5 and 6 respectively. The W=N bond distances of 1.74 Å (average) are similar and characteristic for six-coordinate tungsten imido complexes [42,43]. The $W–O_{Ph}$ distances of

Table 3
Intramolecular bond distances for $W(=NC_6H_3–2,6\text{-}Me_2)Cl_3(Hsal–3\text{-}Me\cdots OEt_2)$ (**4c**). Estimated standard deviations in the least significant figure are given in parentheses

Atoms		Distance (Å)	Atoms		Distance (Å)
W(1)	Cl(1)	2.337(2)	O(1)	C(2)	1.339(8)
W(1)	Cl(2)	2.359(2)	O(2)	C(7)	1.266(8)
W(1)	Cl(3)	2.343(2)	O(3)	C(7)	1.301(9)
W(1)	O(1)	1.916(4)	O(3)	H(26)	1.23[a]
W(1)	O(2)	2.155(4)	N(1)	C(9)	1.381(9)
W(1)	N(1)	1.762(6)			

[a] H(26) was not found in the Fourier difference map, but was arbitrarily placed halfway between O(3) (of the acid) and O(4) (of ether).

Table 4
Intramolecular bond angles for $W(=NC_6H_3–2,6\text{-}Me_2)Cl_3(Hsal–3\text{-}Me\cdots OEt_2)$ (**4c**). Estimated standard deviations in the least significant figure are given in parentheses

Atoms			Angle (deg)	Atoms			Angle (deg)
Cl(1)	W(1)	Cl(2)	86.13(6)	Cl(3)	W(1)	O(1)	92.8(1)
Cl(1)	W(1)	Cl(3)	90.83(7)	Cl(3)	W(1)	O(2)	82.1(1)
Cl(1)	W(1)	O(1)	162.9(1)	Cl(3)	W(1)	N(1)	94.5(2)
Cl(1)	W(1)	O(2)	82.5(1)	O(1)	W(1)	O(2)	81.5(2)
Cl(1)	W(1)	N(1)	98.3(2)	O(1)	W(1)	N(1)	98.1(2)
Cl(2)	W(1)	Cl(3)	165.59(7)	O(2)	W(1)	N(1)	176.6(2)
Cl(2)	W(1)	O(1)	86.2(1)	W(1)	O(1)	C(2)	137.2(4)
Cl(2)	W(1)	O(2)	83.5(1)	W(1)	O(2)	C(7)	132.8(5)
Cl(2)	W(1)	N(1)	99. 8(2)	O(2)	C(7)	O(3)	120.2(6)
W(1)	N(1)	C(9)	176.0(5)				

Table 5
Intramolecular bond distances for $W(=NC_6H_3–2,6\text{-}Me_2)Cl_3$ $(Hsal–3\text{-}Me\cdots NEt_3)$ (**6c**). Estimated standard deviations in the least significant figure are given in parentheses

Atoms		Distance (Å)	Atoms		Distance (Å)
W(1)	Cl(1)	2.367(2)	O(2)	C(7)	1.290(8)
W(1)	Cl(2)	2.341(1)	O(3)	C(7)	1.249(8)
W(1)	Cl(3)	2.376(2)	N(1)	C(9)	1.385(8)
W(1)	O(1)	1.916(4)	N(2)	C(17)	1.521(8)
W(1)	O(2)	2.088(4)	N(2)	C(19)	1.504(9)
W(1)	N(1)	1.737(5)	N(2)	C(21)	1.47(1)
O(1)	C(2)	1.358(7)	N(2)	H(0)	0.716[b]

[b] The proton H(0) was found in the Fourier difference map.

Table 6
Intramolecular bond angles for W(=NC_6H_3-2,6-Me_2)Cl_3 (Hsal-3-Me···NEt_3) (**6c**). Estimated standard deviations in the least significant figure are given in parentheses

Atoms			Angle (deg)	Atoms			Angle (deg)
Cl(1)	W(1)	Cl(2)	88.37(6)	O(1)	W(1)	O(2)	82.6(2)
Cl(1)	W(1)	Cl(3)	86.87(6)	O(1)	W(1)	N(1)	91.3(2)
Cl(1)	W(1)	O(1)	168.4(1)	O(2)	W(1)	N(1)	173.9(2)
Cl(1)	W(1)	O(2)	87.0(1)	W(1)	O(1)	C(2)	134.5(4)
Cl(1)	W(1)	N(1)	98.9(2)	W(1)	O(2)	C(7)	134.4(4)
Cl(2)	W(1)	Cl(3)	166.60(6)	W(1)	N(1)	C(9)	168.9(5)
Cl(2)	W(1)	O(1)	95.7(1)	O(2)	C(7)	O(3)	122.1(6)
Cl(2)	W(1)	O(2)	84.0(1)	C(17)	N(2)	H(0)	105.99[b]
Cl(2)	W(1)	N(1)	97.6(2)	C(19)	N(2)	C21)	115.5(5)
Cl(3)	W(1)	O(1)	86.7(1)	C(17)	N(2)	C(19)	109.6(5)
Cl(3)	W(1)	O(2)	83.2(1)	C(17)	N(2)	C(21)	114.2(6)
Cl(3)	W(1)	N(1)	95.5(2)				

1.916(4) Å are again typical for non-π-donor phenoxides [16,18–20]. The amine O–H···N hydrogen bond distance of 2.677(7) Å is slightly longer than the O–H···O bond 2.512(7) Å of the diethyl ether adduct. Aside from the hydrogen bonds, the most significant structural differences in the complexes are found in the η^1-carboxylate group. The ether and amine structures can be regarded as the superimposition of three possible valence bond forms. The first valence structure (**V**) contains a fully protonated form of the acid, with correspondingly little positive charge localization on the Brønsted base. The second structure (**VI**) exhibits a largely deprotonated acid functionality, with the bulk of the negative charge localized on the non-tungsten bound carboxylate oxygen. The last valence structure (**VII**) has charge separation similar to **VI**, with negative charge localization at the tungsten center. Structure **VII** should possess a stronger bond between the tungsten and carbonyl oxygen, and more double bond character between the carboxylate carbon and the non-tungsten-bound carboxylate oxygen.

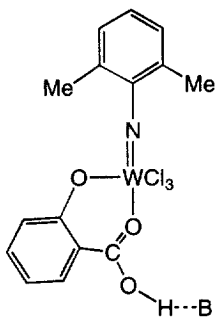

V

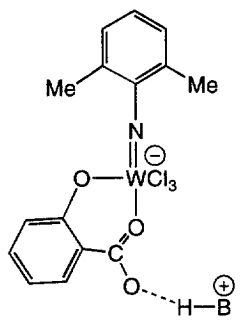

VI

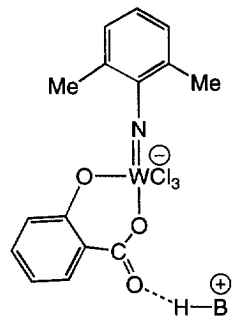

VII

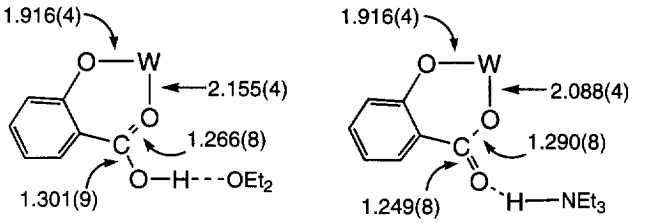

Fig. 3. Graphical comparison of bond distances and angles in the Hsal-3-Me units of **4c** (OEt_2) and **6c** (NEt_3).

Bond distances and angles for the salicylate ligands **4c** and **6c** are illustrated for direct comparison in Fig. 3. Both of these structures, like **3e**, can best be described as a combination of valence forms **V** and **VI**. However, an examination of the bond distances in **4c** and **6c** indicates that the $W–O_{carbonyl}$ and $C_{carbonyl}–O_{OH}$ bonds are shorter in **6c** by 0.067(6) Å and 0.052(6) Å respectively. The $C=O_{carbonyl}$ bond is also correspondingly longer by 0.024(11) Å in **6c**. These trends are indicative of subtle changes in the bonding environment in the triethylamine adducts. Considering that the ether and amine adducts are primarily differentiated by greater charge separation in the amine complex, we might attribute more character from **VI** to **6c**. However, an analogy to **VI** does not entirely account for the structural changes observed in the amine adduct. The virtual equality of the C–O bond lengths in the carboxylate unit of **6c** is indicative of more electronic delocalization than in structures **VI** or **VII** alone. That is to say, **6c** is best represented by a composite of the resonance structures **VI** and **VII**. This hypothesis is confirmed by the accompanying decrease in the $W–O_{carboxyl}$ bond length by ~0.07 Å, which is consistent with a small increase in charge donation to tungsten (like **VII**). Coming from the weakly bonded group trans to the imido ligand, it is not surprising that this increased donation has little effect on the bonding environment of the metal. The W=N distance shows no measurable change between the two complexes, but there is a slight increase (0.02 Å) in the average W–Cl bond distances in the amine complex. All of the variations between bond distances in **4c** and **6c** are characteristic of a slight increase in negative charge localization at tungsten in **6c** compared with **4c**. This suggests that the bonding description of the amine complex (**6c**) should incorporate some component of **VII**. These subtle structural effects illustrate the changes in the electronic environment of the carboxylate ligand that are ultimately responsible for the observed Hammett correlation with carboxylate ^{13}C chemical shift and variations in the hydrogen bonding behavior of the complexes in solution.

2.3. *Hydrogen bonding behavior*

The titration of $W(X)Cl_3$(Hsal–R) complexes with ether in benzene and chloroform solutions results in a successive downfield shift of the carboxylic acid resonance. Fig. 4 is a graphical representation of the ^1H chemical shift data from the titration of several $[W(=O)Cl_3(Hsal–R)]_2$ compounds (R = Me, H, Ph or Cl) with ether. A

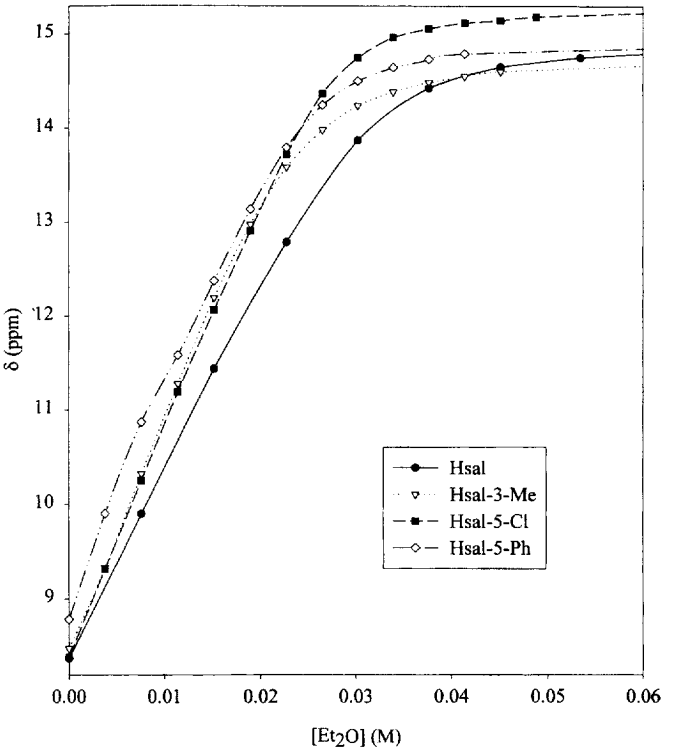

Fig. 4. A plot of $\delta(-CO_2H)$ as a function of ether concentration for the various $[W(=O)Cl_3(Hsal\text{–}R)]_2$ compounds (R = Me, H, Ph or Cl).

similar series of titrations for $[W(=X)Cl_3(Hsal)]_2$ complexes (X = O, NAr or Ph_2C_2) is shown in Fig. 5. Only a single, time-averaged signal is observed for the acidic protons in mixtures of the free acids and the Lewis-base-bound acid species. This observation does not preclude the presence of di- or poly-nuclear aggregates of the ether adduct and free acid, but it does indicate that all relevant intramolecular and intermolecular ether exchange processes must be rapid on the NMR time scale. The linearity of the curves in the early stages of the titrations suggests binding constants greater than unity. Although a linear Scatchard approximation produced an acceptable fit for the binding of ether to mononuclear $W(X)Cl_3(Hcat)$ compounds [16], this solution failed to fit the NMR data for ether binding with $[W(X)Cl_3(Hsal\text{–}R)]_2$ complexes. This is probably an indication that the self-association of $[W(X)Cl_3(Hsal)]_2$ complexes renders the diol–diolate binding model [16] invalid for the Hsal systems.

Two more plausible models for the binding of the ether with $[W(X)Cl_3(Hsal\text{–}R)]_2$ are expressed in Scheme 2. The first model involves predissociation of $[W(X)Cl_3(Hsal\text{–}R)]_2$ into $W(X)Cl_3(Hsal\text{–}R)$ and subsequent reaction of the monomer with the ether. The second presumes the stepwise binding of

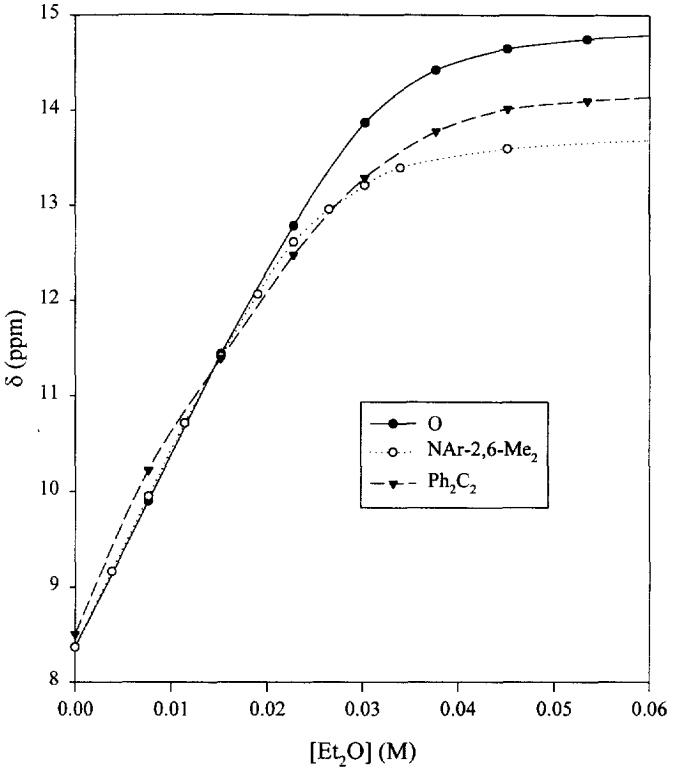

Fig. 5. A plot of $\delta(-CO_2H)$ as a function of ether concentration for $[W(X)Cl_3(Hsal)]_2$ compounds (X = O, NC_6H_3-2,6-Me_2 or Ph_2C_2).

one equivalent of ether to a tungsten dimer, followed by association of a second equivalent of ether and concomitant cleavage of the dimer into mononuclear adducts. Non-linear routines can successfully model this data using either equilibrium system, although only the fit to the second model provides truly meaningful results. The fit to the first model generates dissociation constant values (K_D between 10^{-3} and 5 M^{-1}) that vary randomly with the substitution pattern at both the metal or the Hsal–R unit. Still more troubling is the tendency of this model to generate K_D values that are at odds with the determined solution molecular weights of the complexes.

The second model generates ether binding constants that are readily reconciled with observed chemistry of the systems. The data collected in Table 7 represent the first association constants K_1 of ether with various free acid species. These K_1 values were determined by plotting δ versus [L] and evaluating the initial slope of the function as

$$\text{initial slope} = d\delta/d[L] = K_1\delta_{M_2L}(1 + K_1M_{2o})^{-1} \text{ for the condition } \lim [L] \rightarrow 0$$

where δ is the observed chemical shift, δ_{M_2L} is the calculated chemical shift of a mono-ether adduct intermediate, M_{2o} is the initial M_2 concentration, [L] is the

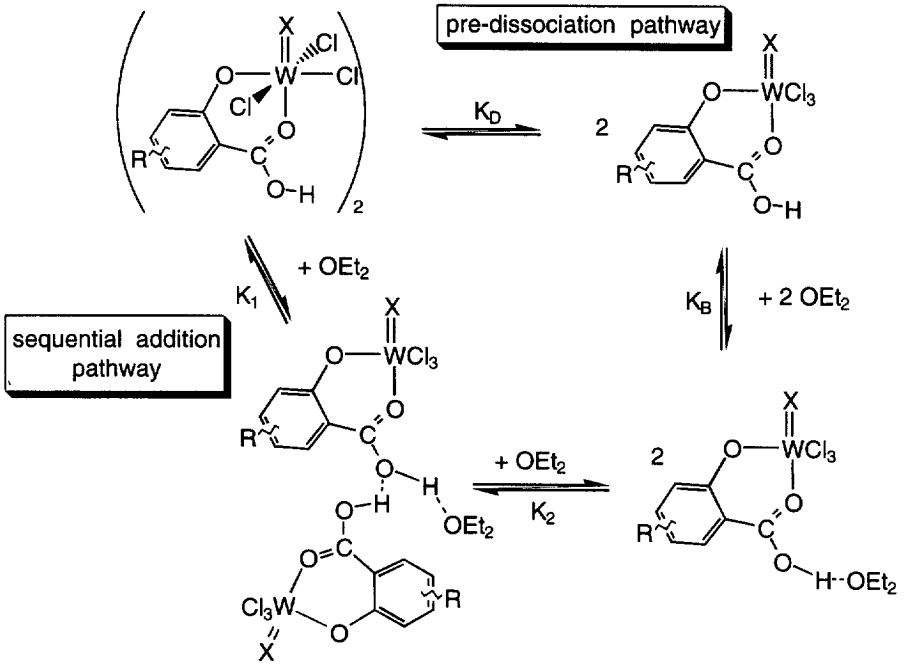

Scheme 2. Possible equilibria in the titration of salicylate free acids.

Table 7
Ether association constants K_1 for $[W(X)Cl_3(Hsal\text{–}R)]_2$ complexes

$[W(X)Cl_3(Hsal\text{–}R)]_2$ complex		K_1 (M^{-1})
$[W(=O)Cl_3(Hsal\text{–}3\text{-}Me)]_2$	**1c**	31
$[W(=O)Cl_3(Hsal)]_2$	**1a**	25
$[W(=O)Cl_3(Hsal\text{–}5\text{-}Ph)]_2$	**1d**	28
$[W(=O)Cl_3(Hsal\text{–}5\text{-}Cl)]_2$	**1b**	20
$[W(=NC_6H_3\text{–}2,6\text{-}Me_2)Cl_3(Hsal)]_2$	**2a**	27
$[W(=NC_6H_3\text{–}2,6\text{-}Me_2)Cl_3(Hsal\text{–}5\text{-}Cl)]_2$	**2b**	18
$[W(\eta^2\text{-}Ph_2C_2)Cl_3(Hsal)]_2$	See Ref. [17]	19
$[W(\eta^2\text{-}Ph_2C_2)Cl_3(Hsal\text{–}5\text{-}Cl)]_2$	See Ref. [17]	23

concentration of ether added, and K_1 is the first ether binding constant. The resulting K_1 values represent modestly thermodynamically favorable association constants, varying between 18 and 31. Errors in these measurements are large, amounting to $\pm 10\%$ of the total value. Some trends can be identified in these data: (1) Binding constants vary over a relatively small range, considering the potential electronic variation induced by the substituents on the tungsten center and the salicylate moiety. (2) Ether binding constants for the tungsten oxo Hsal–R compounds generally correlate with the Hammett parameters of the substituents [32–34]. The Hammett correlation has a negative slope, indicating that decreased negative charge

density on the carboxylate ligand results in a reduced binding affinity for ether. (3) The magnitude of the binding constants for the oxo and aryl imido systems are very similar and show the same general dependence on the electron-withdrawing characteristics of R. This suggests that there is significant similarity in the electronic effects exerted by the oxo and aryl imido ligands, which are both formally six electron donor dianions. (4) The ether binding constants for the diphenylacetylene complexes are small and are probably identical within experimental error. The fact that both the $[W(Ph_2C_2)Cl_3(Hsal)]_2$ and $[W(Ph_2C_2)Cl_3(Hsal\text{–}5\text{-}Cl)]_2$ complexes are relatively weak ether acceptors is characteristic of the poor hydrogen bonding ability of these compounds (as noted above; also, see Table 7).

These trends are complicated by the nature of the equilibrium under investigation (Scheme 2). K_1 is a measure of the first ether binding constant, which involves ether association with the hydrogen-bonded dimer. The binding event probably involves some structural reorganization, and may even result in the scission of intramolecular hydrogen bonds in order to accommodate hydrogen bonding to the ether moiety. This reorganization probably reduces the thermodynamic favorability of ether binding. Moreover, substitutional variations that reduce the strength of intramolecular hydrogen bonding in the $[W(X)Cl_3(Hsal\text{–}R)]_2$ dimers are likely to exert similar effects in the related $W(X)Cl_3(Hsal\text{–}R\cdots OEt_2)$ complexes. This probably accounts for the small range of K_1 values observed for the variety of tungsten complexes studied.

The titration of $[W(X)Cl_3(Hsal\text{–}R)]_2$ with triethylamine in benzene-d_6 yields spectra that are consistent with those observed during ether titrations. During the amine titrations, there is rapid exchange between the acidic protons on residual free acid and the triethylammonium ion of the $W(X)Cl_3(Hsal\text{–}R\cdots NEt_3)$ salts. Spectroscopic studies of titrations with triethylamine in purified $CDCl_3$ proved more complicated than those performed in benzene. During the titration, acidic proton resonances appeared that were not in rapid equilibrium with either the $[W(X)Cl_3(Hsal)]_2$ starting material or its trialkylammonium salt. This is probably not caused by the presence of an intermediate hydrogen-bonded aggregate like $[W(=O)Cl_3(Hsal)]_2\cdots(NEt_3)$, because intramolecular proton exchange in such a species should be rapid. Instead, the presence of multiple acidic proton resonances suggests that chemically distinct species are formed during the titration of the metal complex. The new product could be a new metal complex that exhibits slow chemical exchange with the salicylate complexes, although this seems unlikely as no distinctly new tungsten complexes are observed spectroscopically. Furthermore, no new metal-containing species are isolated from these reaction systems. It seems most likely that these new acidic proton resonances are generated through $CDCl_3$ association with triethylamine, resulting in the formation of a distinct hydrogen bonding moiety (such as ammonium chloride) in the titration medium [44].

3. Conclusions

Salicylate complexes of $W(X)Cl_3$ templates, where X is O, NC_6H_3–2,6-Me_2 or Ph_2C_2, are formed in reactions with $W(X)Cl_4$ precursors. The products are robust

inorganic and organometallic free-acids that favor coordination of the carboxylic acid through the carbonyl oxygen and trans to the X group. The complexes associate in solution to form dimers, although the mode of association is not known. Given the fact that carboxylic acids are good hydrogen bond donors, it seems likely that the molecules aggregate by hydrogen bonding with chlorides on adjacent molecules. This O–H···Cl mode of hydrogen bonding would be preferred because the carbonyl oxygen is (1) more sterically crowded owing to metal binding and (2) less basic owing to electron donation to the metal. The addition of more electron-donating substituents to the salicylate ligand shows small effects on the strength of hydrogen bonding interactions, increasing the binding affinity of a single ether molecule to form a $[W(X)Cl_3(Hsal–R)]_2\cdots(OEt_2)$ intermediate. A noteworthy decrease in ether binding affinity is observed as the π-donating ability of X is increased: $O \geqslant NC_6H_3$–2,6-$Me_2 > Ph_2C_2$. These results indicate that variations in either the substitution pattern at the metal or in substituents on the Hsal unit may be useful in tuning the hydrogen bond affinity of these and related inorganic free-acid complexes. Current studies in our laboratory are seeking applications of these subunits in materials synthesis and catalysis.

4. Experimental

All experiments were performed under a nitrogen atmosphere in an HE-553-2 Vacuum Atmospheres dry box or using standard Schlenk techniques. Hexane, toluene, dimethoxyethane (dme), and diethyl ether were purified by distillation over Na/benzophenone. Dichloromethane and triethylamine were purified by distillation over CaH_2, followed by purging with dry nitrogen. NMR solvents (Cambridge Isotope Laboratories) were dried with 5 Å molecular sieves and degassed with dry nitrogen prior to use. Salicylic acid (H_2sal), 5-chlorosalicylic acid (H_2sal–5-Cl), 3-methylsalicylic acid (H_2sal–3-Me), 2,6-dihydroxybenzoic acid (H_2sal–6-OH) and pamoic acid (H_4pam) were used as-received (Aldrich). Practical-grade 5-phenylsalicylic acid (H_2sal–5-Ph, Eastman–Kodak) was recrystallized from hot toluene, washed with pentane and dried for 1 h at 60°C (10^{-7} Torr). $W(=NC_6H_3$–2,6-$Me_2)Cl_4$ was prepared using published procedures [25,26]. $WOCl_4$ was received as a gift from Hercules Research Company. NMR spectra were recorded on Bruker AM-500 or DRX-400, Varian XL-300, or General Electric QE-300 spectrometers at ambient temperature (~20°C) unless otherwise noted. ^1H and ^{13}C data are listed in parts per million (ppm) downfield from tetramethylsilane, with ^1H data referenced against the residual solvent proton peak. All coupling constants J listed are in hertz. Elemental analyses were performed by Desert Analytics (PO Box 41838, Tucson, AZ 85717).

4.1. *W(=O)Cl$_3$(Hsal) (1a)*

$WOCl_4$ (10.111 g, 29.59 mmol) was slurried in 250 ml of dichloromethane in a 500 ml Schlenk flask equipped with a stir bar. Salicylic acid (4.089 g, 29.60 mmol)

was added slowly to the slurry, noting the change from bright orange to deep crimson. If the acid is added too quickly, the dichloromethane will boil owing to the exothermic nature of the reaction. The mixture was stirred for 20 h, followed by the removal of solvent in vacuo. The dark red solid was triturated in ~80 ml of hexane, then filtered. The hexane was discarded and the red powder dried in vacuo for several hours. Yield: 93% (12.155 g, 27.42 mmol). NMR data ($CDCl_3$, 300 MHz): ^1H, δ 8.56 (H, bs, $-CO_2H$), 8.30 (H, dd, $J_{5-6}=7.9$, $J_{4-6}=1.6$, 6-H of Hsal), 7.93 (H, t, 4-H of Hsal), 7.39 (H, t, 5-H of Hsal), 7.21 (H, d, $J_{3-4}=8.6$, 3-H of Hsal); ^{13}C, δ 170.05 ($-CO_2H$), 160.68, 138.20, 132.43, 129.20, 122.87, 116.94. Analytical data for $C_7H_5O_4WCl_3$. Calc. 18.97% C, 1.14% H. Actual 19.15% C, 1.04% H.

4.2. *W(=O)Cl$_3$(Hsal-5-Cl) (**1b**)*

This dark red compound was prepared in the same manner as **1a** using 5-chlorosalicylic acid (5.530 g, 32.05 mmol) and $WOCl_4$ (10.950 g, 32.05 mmol). Yield: 87% (13.260 g, 27.8 mmol). NMR data ($CDCl_3$, 300 MHz): ^1H, δ 8.60 (1H, bs, $-CO_2H$), 8.23 (1H, d), 7.85 (1H, dd), 7.17 (1H, d); ^{13}C, δ 169.2 ($-CO_2H$), 159.3, 137.9, 134.8, 131.8, 124.3, 117.9. Analytical data for $C_7H_4O_4WCl_4$. Calc.: 17.60% C; 0.84% H. Found: 17.22% C; 0.78% H.

4.3. *W(=O)Cl$_3$(Hsal-3-Me) (**1c**)*

This dark red compound was prepared in the same manner as **1a** using 3-methylsalicylic acid (4.875 g, 32.04 mmol) and $WOCl_4$ (10.947 g, 32.04 mmol). Yield: 73% (10.387 g, 23.53 mmol). NMR data ($CDCl_3$, 300 MHz): ^1H, δ 8.33 (1H, bs, $-CO_2H$), 8.13 (1H, d), 7.79 (1H, d), 7.25 (1H, t), 2.59 (3H, s, sal-3-CH_3); ^{13}C, δ 170.37 ($-CO_2H$), 155.81, 139.60, 133.39, 130.29, 128.87, 116.89, 16.07 (sal-3-CH_3). Analytical data for $C_8H_7O_4WCl_3$. Calc.: 21.01% C; 1.54% H. Found: 21.22% C; 1.47% H.

4.4. *W(=O)Cl$_3$(Hsal-5-Ph) (**1d**)*

5-Phenylsalicylic acid was added to a slurry of $WOCl_4$ (1.158 g, 3.39 mmol) in 30 ml of hexane. The mixture was stirred for 13 h, then washed with a hexane/dichloromethane solution (20 ml and 3 ml respectively). The bluish-purple powder was dried for 10 h at room temperature (10^{-7} Torr). Yield: 86% (1.522 g, 2.93 mmol). NMR data ($CDCl_3$, 300 MHz): ^1H, δ 8.69 (H, bs, $-CO_2H$), 8.47 (H, d, $J_{4-6}=8.7$, 6-H of Hsal–5-Ph), 8.10 (H, dd, $J_{3-4}=8.6$, 4-H of Hsal–5-Ph), 7.59 (2H, d, $J=7.0$, *o*-H of Ph), 7.53 (2H, t, $J=7.3$, *m*-H of Ph), 7.44 (H, t, $J=7.0$, 4-H of Ph), 7.27 (H, d, 3-H of Hsal–5-Ph); ^{13}C, δ 169.99 ($-CO_2H$), 169.80, 159.99, 142.80, 137.38, 136.06, 130.55, 129.29, 127.39, 123.51, 117.45.

4.5. $W(=NC_6H_3\text{–}2,6\text{-}Me_2)Cl_3(Hsal)$ (**2a**)

$W(=NC_6H_3\text{–}2,6\text{-}Me_2)Cl_4$ (3.485 g, 7.83 mmol) was slurried in 15 ml of dichloromethane and 30 ml of hexane in a 50 ml Schlenk flask. Salicylic acid (1.082 g, 7.83 mmol) was added via addition tube and the mixture stirred for 36 h. The reaction darkened to a brownish-red color and, as the reaction proceeded, a metallic gray, microcrystalline product precipitated. The volume of the slurry was reduced to ~25 ml, then filtered. The precipitate was then dried under high vacuum for 24 h. Yield: 92% (3.934 g, 7.20 mmol). NMR ($CDCl_3$, 300 MHz): ^1H, δ 8.40 (H, very bs, $-CO_2H$), 8.23 (H, dd, $J_{5-6}=8.0$, $J_{3-5}=1.6$, 6-H of Hsal), 7.83 (H, dd, $J_{3-4}=7.0$, $J_{3-5}=1.7$, 3-H of Hsal), 7.29 (3H, d, $J_o=7.7$, 3,5-H of imido overlapping triplet of 4-H of Hsal), 7.08 (H, d, $J_{3-4}=8.0$, 3-H of Hsal), 6.71 (H, t, $J_o=7.7$, 4-H of imido), 3.22 (6H, s, NAr–2,6-(CH_3)$_2$); ^{13}C, δ 171.36 ($-CO_2H$), 162.76, 149.25, 144.35, 138.57, 132.34, 132.10, 126.45, 125.84, 122.04, 114.21, 18.02 (NAr–2,6-(CH_3)$_2$). Analytical data for $C_{15}H_{14}NO_3WCl_3$. Calc.: 32.97% C, 2.58% H, 2.56% N. Found: 32.66% C, 2.45% H, 2.38% N.

4.6. $W(=NC_6H_3\text{–}2,6\text{-}Me_2)Cl_3(Hsal\text{–}5\text{-}Cl)$ (**2b**)

This metallic gray compound was prepared in the same manner as **2a** using 5-chlorosalicylic acid (1.196 g, 6.93 mmol) and $W(=NC_6H_3\text{–}2,6\text{-}Me_2)Cl_4$. Yield: 84% (3.371 g, 5.80 mmol). NMR ($CDCl_3$, 300 MHz): ^1H, δ 8.59 (1H, bs, $-CO_2H$), 8.17 (1H, s), 7.73 (1H, d), 7.30 (2H, d), 7.03 (1H, d), 6.69 (1H, t), 3.23 (6H, s, NAr–2,6-(CH_3)$_2$); ^{13}C, δ 170.6 ($-CO_2H$), 161.2, 149.2, 144.4, 138.2, 132.5, 131.3, 131.1, 126.3, 123.5, 116.6, 115.9, 18.0 (NAr–2,6-(CH_3)$_2$). Analytical data for $C_{15}H_{13}NO_3WCl_4$. Calc.: 31.01% C; 2.26% H; 2.41% N. Found: 31.29% C; 1.97% H; 2.38% N.

4.7. $W(=NC_6H_3\text{–}2,6\text{-}Me_2)Cl_3(Hsal\text{–}3\text{-}Me)$ (**2c**)

This compound was synthesized in a manner similar to **1a**. $W(=NAr\text{–}2,6\text{-}Me_2)Cl_4$ (4.271 g, 9.60 mmol) was slurried in 50 ml of dichloromethane and stirred for 2 days with 3-methylsalicylic acid (1.461 g, 9.60 mmol). The volume of the mixture was reduced in vacuo to ~25 ml, then cold-filtered. The metallic gray, microcrystalline product was washed with hexane (2 × 15 ml), then dried in vacuo (10^{-6} Torr) for 3 h. Yield: 86% (4.652 g, 8.29 mmol). NMR ($CDCl_3$, 300 MHz): ^1H, δ 8.33 (1H, bs, $-CO_2H$), 8.08 (1H, d), 7.71 (1H, d), 7.28 (2H, d), 7.17 (1H, t), 6.68 (1H, t), 3.23 (6H, s, NAr–2,6-(CH_3)$_2$), 2.43 (3H, s, sal–3-CH_3); ^{13}C (partial), δ 172.07 ($-CO_2H$), 161.90, 149.60, 143.26, 140.36, 132.12, 130.35, 126.82, 125.94, 114.38, 18.42 (NAr–2,6-(CH_3)$_2$), 17.35 (sal–3-CH_3). Analytical data for $C_{16}H_{16}O_3WCl_3$. Calc.: 34.29% C; 2.88% H; 2.50% N. Found: 33.97% C; 2.81% H; 2.51% N.

4.8. $W(=NAr\text{–}2,6\text{-}Me_2)Cl_3(Hsal\text{–}5\text{-}Ph)$ (**2d**)

$W(=NAr\text{–}2,6\text{-}Me_2)Cl_4$ (1.459 g, 3.28 mmol) was stirred for 5 h with 5-phenylsalicylic acid (0.6921 g, 3.23 mmol) in 30 ml of dichloromethane. The volume of the solution was reduced in vacuo, then layered with 10 ml of hexane. The flask was cooled to −20°C and yielded lustrous purple block crystals. More crystals were harvested upon further treatment of the mother liquor with hexane. Yield: 56% (1.152 g, 1.85 mmol). NMR data ($CDCl_3$, 300 MHz): ^1H, δ 8.5 (H, very broad s, $-CO_2H$), 8.41 (H, d, $J_{4\text{–}6}=8.6$, 6-H of Hsal–5-Ph), 8.03 (H, dd, 4-H of Hsal–5-Ph), 7.59 (2H, d, $J=8.0$, *o*-H of Ph), 7.51 (2H, t, $J=7.0$, *m*-H of Ph), 7.42 (H, t, $J=7.0$, 4-H of Ph), 7.29 (2H, d, $J=7.8$, *o*-H of imido), 7.15 (H, d, 3-H of *Hsal*–5-Ph), 6.71 (H, t, 4-H of imido), 3.22 (6H, s, NAr–2,6-$(CH_3)_2$); ^{13}C (partial), δ 171.22 ($-CO_2H$), 162.00, 144.32, 139.39, 138.19, 136.89, 132.32, 130.20, 129.19, 128.58, 127.11, 126.45, 122.61, 114.46, 18.10 (NAr–2,6-$(CH_3)_2$). Analytical data for $C_{21}H_{18}NO_3WCl_3$. Calc. 40.51% C, 2.91% H, 2.25% N. Found 40.69% C, 2.87% H, 2.32% N.

4.9. $W(=O)Cl_3(Hsal\cdots OEt_2)$ (**3a**)

In a small Schlenk flask, $WOCl_4$ (0.39 g, 1.14 mmol) was dissolved in dry Et_2O. To the orange solution, salicylic acid (0.1575 g, 1.14 mmol) was added via addition tube. The magnetically stirred mixture became dark red instantaneously. After 12 h the solvent was removed in vacuo. The red powder is infinitely soluble in any solvent applied and thus did not crystallize. Yield: 77.6% (0.453 g, 0.88 mmol). NMR data ($CDCl_3$, 300 MHz): ^1H, δ 14.45 (1H, bs, $-CO_2H\cdots OEt_2$), 8.25 (1H, d), 7.82 (1H, t), 7.32 (1H, t), 7.16 (1H, d), 3.81 (4H, q, $O(CH_2CH_3)_2$), 1.32 (6H, t, $O(CH_2CH_3)_2$); ^{13}C, δ 171.0 ($-CO_2H\cdots OEt_2$), 160.0, 136.8, 132.1, 129.0, 127.0, 122.6, 66.5 ($O(CH_2CH_3)_2$), 14.5 ($O(CH_2CH_3)_2$). Analytical data for $C_{11}H_{15}O_5WCl_3$. Calc.: 25.53%C; 2.92%H. Found: 25.19% C; 2.82% H.

4.10. $W(=O)Cl_3(Hsal\text{–}5\text{-}Cl\cdots OEt_2)$ (**3b**)

This dark red compound was prepared in the same manner as **3a** using 5-chlorosalicylic acid. NMR ($CDCl_3$, 300 MHz): ^1H, δ 15.15 (1H, s, $-CO_2H\cdots OEt_2$), 8.21 (1H, s), 7.77 (1H, d), 7.12 (1H, d), 3.87 (4H, q, $O(CH_2CH_3)_2$), 1.34 (6H, t, $O(CH_2CH_3)_2$); ^{13}C, δ 170.12 ($-CO_2H\cdots OEt_2$), 158.71, 136.43, 134.50, 131.45, 123.86, 119.72, 66.51 ($O(CH_2CH_3)_2$) 14.22 ($O(CH_2CH_3)_2$).

4.11. $W(=O)Cl_3(Hsal\text{–}3\text{-}Me\cdots OEt_2)$ (**3c**)

This dark red compound was prepared in the same manner as **3a** using 3-methylsalicylic acid. Yield: 88% (0.78 g, 1.47 mmol). NMR data ($CDCl_3$, 300 MHz): ^1H, δ 14.21 (1H, bs, $-CO_2H\cdots OEt_2$), 8.11 (1H, d), 7.72 (1H, d), 7.19 (1H, t), 3.82 (4H, q, $O(CH_2CH_3)_2$), 2.58 (3H, s, sal–3-CH_3), 1.32 (6H, t, $O(CH_2CH_3)_2$); ^{13}C, δ 171.0 ($-CO_2H\cdots OEt_2$), 160.0, 138.2, 133.0, 129.9, 128.7, 119.0,

66.5 ($O(CH_2CH_3)_2$), 16.0 (sal–3-CH_3), 14.5 ($O(CH_2CH_3)_2$). Analytical data for $C_{12}H_{17}O_5WCl_3$. Calc.: 27.12% C; 3.22% H. Found: 27.33% C; 3.19% H.

4.12. *[W(=O)Cl$_3$(Hsal)]$_2$···(dme) (3e)*

$WOCl_4$ (2.451 g, 7.17 mmol) and a magnetic stir bar were placed into a 50 ml Schlenk flask and slurried in 25 ml of dichloromethane. In a separate flask, salicylic acid (0.990 g, 7.17 mmol) was dissolved with dimethoxyethane (0.39 ml, 3.73 mmol) and 25 ml of dichloromethane. The salicylic acid solution was added to the stirred $WOCl_4$ slurry via cannula, resulting in a change from its typical bright orange color to a deep red slurry. In about 20 min all the material had dissolved. The volume was reduced in vacuo and the solution cooled to −20°C. The deeply colored black crystals harvested were suitable for X-ray diffraction analysis. Yield: 84% (2.954 g, 3.02 mmol). NMR data ($CDCl_3$, 300 MHz): ^{1}H, δ 12.09 (2H, bs s, –CO_2H···dme), 8.25 (2H, d), 7.86 (2H, t), 7.32 (2H, t), 7.16 (2H, d), 3.92 ($(CH_3OCH_2)_2$), 3.62 ($(CH_3OCH_2)_2$); ^{13}C, δ 170.89 (–CO_2H···dme), 160.38, 137.36, 132.28, 129.23, 122.63, 118.03, 70.94 (($CH_3OCH_2)_2$), 59.14 (($CH_3OCH_2)_2$). Analytical data for $C_{18}H_{20}O_{10}W_2Cl_6$. Calc.: 22.13% C, 2.06% H. Found: 22.23% C, 1.82% H.

4.13. *[W(=O)Cl$_3$](H$_2$pam···1.5OEt$_2$) (3f)*

This indigo-colored compound was prepared in a manner similar to **3a**, using two equivalents of $WOCl_4$ (1.547 g, 4.53 mmol) and one equivalent of pamoic acid (0.874 g, 2.25 mmol) in 40 ml of Et_2O. The mixture was refluxed for 12 h, cooled and filtered. The precipitate was dried in vacuo for 3 h. Yield: 79% (1.982 g, 1.78 mmol). NMR data ($CDCl_3$, 300 MHz): ^{1}H, δ 14.12 (2H, bs, –OH···OEt_2), 8.80 (2H, s), 8.26 (2H, d, J=8.6), 8.04 (2H, d, J=8.3), 7.76 (2H, t, J=7.6 Hz), 7.51 (2H, t, J=7.4), 5.62 (2H, s, CH_2 bridge), 3.73 (8H, q, $(CH_3CH_2)_2O$), 1.28 (12H, t, $(CH_3CH_2)_2O$); ^{13}C, δ 171.5 (carboxyl), 153.6, 135.8, 135.0, 132.8, 132.0, 131.4, 130.9, 129.3, 126.6, 116.1, 66.4 ($O(CH_2CH_3)_2$), 29.7 (CH_2 bridge), 14.6 ($O(CH_2CH_3)_2$). Analytical data for $C_{29}H_{29}O_{9.5}W_2Cl_6$. Calc.: 31.38% C, 2.63% H. Found: 31.45% C, 2.61% H.

4.14. *W(=O)Cl$_3$(Hsal–6-(OH)···OEt$_2$) (3g)*

This dark red compound was prepared in the same manner as **1** using 2,6-dihydroxybenzoic acid. Yield: 89% (0.71 g, 1.33 mmol). NMR data ($CDCl_3$, 300 MHz): ^{1}H, δ 14.33 (1H, bs, –OH···OEt_2), 7.69 (1H, t), 6.85 (1H, d), 6.65 (1H, d), 3.82 (4H, q, $O(CH_2CH_3)_2$), 1.32 (6H, t, $O(CH_2CH_3)_2$). Analytical data for $C_{11}H_{15}O_6WCl_3$. Calc.: 24.77% C; 2.83% H. Found: 24.23% C; 2.78% H.

4.15. *W(=NC$_6$H$_3$–2,6-Me$_2$)Cl$_3$(Hsal···OEt$_2$) (4a)*

A Schlenk flask equipped with a magnetic stirbar was charged with **2a** (1.049 g, 1.92 mmol). The material was dissolved in 30 ml of Et_2O and stirred for 30 min.

The solution was filtered through a fine frit, the volume reduced to ~20 ml in vacuo, then cooled to −20°C. Reddish-brown needles crystallized from the solution after standing for several hours. Yield: 89% (1.062 g, 1.71 mmol). NMR ($CDCl_3$, 300 MHz): ^1H, δ 12.73 (H, very bs, $-CO_2H\cdots OEt_2$), 8.21 (H, dd, $J_{5-6}=7.9$, $J_{4-6}=1.6$, 6-H of Hsal), 7.74 (H, dd, $J_o=7.9$, 5-H of Hsal), 7.27 (2H, d, $J_o=7.7$, 3,5-H of imido overlapping triplet of 5-H of Hsal), 7.23 (H, dd, $J_o=7.8$, 4-H of Hsal), 7.02 (H, d, $J_o=8.3$, 3-H of Hsal), 6.68 (H, t, $J_o=7.7$, 4-H of imido), 3.86 (4H, q, $J=7.1$, $O(CH_2CH_3)_2$), 3.21 (3H, s, NAr–2,6-$(CH_3)_2$), 1.35 (6H, t, $J=7.1$, $O(CH_2CH_3)_2$); ^{13}C (partial), δ 172.08 ($-CO_2H\cdots OEt_2$), 162.18, 149.05, 144.29, 137.35, 131.95, 126.37, 125.76, 121.80, 115.82, 66.49 ($O(CH_2CH_3)_2$), 18.09 (NAr–2,6-$(CH_3)_2$), 14.59 ($O(CH_2CH_3)_2$). Analytical data for $C_{21}H_{29}N_2O_3WCl_3$. Calc.: 36.77% C, 3.90% H, 2.26% N. Found: 36.83% C, 3.71% H, 2.19% N.

4.16. $W(=NC_6H_3$–2,6-$Me_2)Cl_3(Hsal$–5-$Cl\cdots OEt_2)$ (**4b**)

This dark red compound was prepared in the same manner as **4a** using 5-chlorosalicylic acid. NMR data ($CDCl_3$, 300 MHz): ^1H, δ 15.22 (1H, s, $-CO_2H\cdots OEt_2$), 8.16 (1H, s), 7.63 (1H, d), 7.27 (2H, d), 7.00 (1H, d), 6.67 (1H, d), 6.67 (1H, t), 3.89 (4H, q, OCH_2CH_3), 3.21 (6H, s, NAr–2,6-$(CH_3)_2$), 1.37 (6H, t, OCH_2CH_3); ^{13}C, δ 171.16 ($-CO_2H\cdots OEt_2$), 160.60, 148.77, 144.05, 136.91, 132.03, 131.00, 130.63, 126.26, 123.21, 116.86, 66.44 ($O(CH_2CH_3)_2$), 17.91 (NAr–2,6-$(CH_3)_2$), 14.38 ($O(CH_2CH_3)_2$).

4.17. $W(=NC_6H_3$–2,6-$Me_2)Cl_3(Hsal$–3-$Me\cdots OEt_2)$ (**4c**)

In a small Schlenk flask under nitrogen, $W(=NC_6H_3$–2,6-$Me_2)Cl_4$ (1.112 g, 2.50 mmol) was slurried in Et_2O. To the mixture, 3-methylsalicylic acid (0.3804 g, 2.50 mmol) was added via an addition tube at ambient temperature. The magnetically stirred mixture turned brown while all of the starting material dissolved. After 12 h the solvent was removed in vacuo. Although the brown powder compound is almost as soluble as its oxo analog, the compound was successfully recrystallized from diethyl ether. Yield: 88.2% (1.405 g, 2.20 mmol). NMR ($CDCl_3$, 300 MHz): ^1H, δ 14.18 (1H, s, $-CO_2H\cdots OEt_2$), 8.06 (1H, d), 7.61 (1H, d), 7.27 (2H, d), 7.12 (1H, t), 6.67 (1H, t), 3.82 (4H, q, $O(CH_2CH_3)_2$), 3.23 (6H, s, NAr–2,6-$(CH_3)_2$), 2.42 (3H, s, sal–3-CH_3), 1.33 (6H, t, $O(CH_2CH_3)_2$); ^{13}C, δ 172.30 ($-CO_2H\cdots OEt_2$), 161.17, 149.12, 142.82, 138.93, 131.42, 131.38, 129.80, 126.38, 125.36, 115.41, 66.31 ($O(CH_2CH_3)_2$), 29.70, 18.04 (NAr–2,6-$(CH_3)_2$), 16.94 (sal–3-CH_3), 14.73 ($O(CH_2CH_3)_2$). Analytical data for $C_{20}H_{26}NO_4WCl_3$. Calc.: 37.85% C; 4.13% H. Found: 36.02% C; 3.79% H.

4.18. $W(=O)Cl_3(Hsal\cdots NEt_3)$ (**5a**)

This orange compound was prepared by adding a triethylamine solution (0.33 ml, 2.36 mmol in 20 ml hexane) to **1b** (1.039 g, 2.34 mmol) slurried in ~10 ml of

dichloromethane. The reaction was stirred for 12 h and the product filtered off. Yield: 76% (0.969 g, 1.78 mmol). NMR data ($CDCl_3$, 300 MHz): ^1H, δ 10.78 (H, bs, $-CO_2H\cdots NEt_3$), 8.21 (H, d, $J_{5-6}=7.4$, 6-H of Hsal), 7.63 (H, t, $J_{3-4}=8.1$, 4-H of Hsal), 7.20 (H, t, 5-H of Hsal), 7.02 (H, d, 3-H of Hsal), 3.29 (6H, d, $J_{HH}=6.2$, $N(CH_2CH_3)_3$), 1.38 (9H, t, $N(CH_2CH_3)_3$); ^{13}C, δ 168.71 ($-CO_2H\cdots NEt_3$), 159.92, 133.18, 131.68, 129.16, 123.46, 122.02, 46.40 ($N(CH_2CH_3)_3$), 9.09 ($N(CH_2CH_3)_3$).

4.19. $W(=O)Cl_3(Hsal\text{-}5\text{-}Cl\cdots NEt_3)$ (**5b**)

This dark red compound was prepared in the same manner as **5a**. Yield: 75% (1.001 g, 1.73 mmol). NMR data ($CDCl_3$, 300 MHz): ^1H, δ 10.12 (1H, bs, $-CO_2H\cdots NEt_3$), 8.10 (1H, s), 7.50 (1H, d), 6.90 (1H, d), 3.20 (6H, m, $N(CH_2CH_3)_3$), 1.33 (9H, t, $N(CH_2CH_3)_3$); ^{13}C, δ 167.56 ($-CO_2H\cdots NEt_3$), 158.41, 134.81, 133.04, 131.45, 124.61, 123.49, 46.65 ($N(CH_2CH_3)_3$), 9.18 ($N(CH_2CH_3)_3$).

4.20. $W(=O)Cl_3(Hsal\text{-}3\text{-}Me\cdots NEt_3)$ (**5c**)

In a small Schlenk flask under nitrogen, **1c** (1.1434 g, 2.50 mmol) was dissolved in 40 ml of dichloromethane. To the red solution, triethylamine (347.5 μl, 2.50 mmol) was added dropwise via syringe at ambient temperature. After 2 h the solvent was removed in vacuo. Yield: 85% (1.04 g, 1.86 mmol). NMR ($CDCl_3$, 400 MHz): ^1H, δ 10.73 (1H, bs, $-CO_2H\cdots NEt_3$), 8.05 (1H, d), 7.50 (1H, d), 7.05 (1H, t), 3.27 (6H, m, $N(CH_2CH_3)_3$), 2.56 (3H, s, sal-3-CH_3), 1.32 (9H, m, $N(CH_2CH_3)_3$); ^{13}C, δ 169.49 ($-CO_2H\cdots NEt_3$), 159.34, 135.03, 132.44, 129.86, 129.13, 123.86, 46.76 ($N(CH_2CH_3)_3$), 16.38 (sal-3-CH_3), 9.30 ($N(CH_2CH_3)_3$). Analytical data for $C_{14}H_{22}NO_4WCl_3$. Calc.: 30.11% C; 3.97% H. Found: 29.80% C; 3.92% H.

4.21. $W(=NC_6H_3\text{-}2,6\text{-}Me_2)Cl_3(Hsal\cdots NEt_3)$ (**6a**)

A weighed quantity of **2a** (0.738 g, 1.35 mmol) was transferred to a Schlenk flask equipped with a magnetic stirbar, then dissolved in 20 ml of dichloromethane. In a separate flask, triethylamine (0.138 g, 1.36 mmol) and 20 ml of hexane were combined. The triethylamine solution was added to the solution of **2a** over 30 min. The evolution of white fumes was observed, more so at the beginning of the addition than towards the end. The solution was stirred for another 30 min, then filtered through a fine frit. The volume was reduced to ~20 ml in vacuo and allowed to stand for several hours, yielding black block crystals. Yield: 82% (0.719 g, 1.11 mmol). NMR ($CDCl_3$, 300 MHz): ^1H, δ 11.30 (H, bs, $-CO_2H\cdots NEt_3$), 8.18 (H, dd, $J_{5-6}=7.6$, $J_{4-6}=1.8$, 6-H of Hsal), 7.53 (H, dd, $J_{3-4}=6.9$, $J_{4-5}=6.6$, $J_{4-6}=1.8$, 4-H of Hsal), 7.23 (2H, d, $J_o=7.5$, 3,5-H of imido), 7.13 (H, dd, $J_{5-6}=7.6$, $J_{4-5}=6.6$, 5-H of Hsal), 6.93 (H, d, $J_{3-4}=6.9$, $J_{3-5}=1.1$, 3-position Hsal), 6.62 (H, t, $J=7.5$, 4-H imido), 3.38 (6H, d of q, $J_{HH}(-CH_2N\cdots HO_2C)=4.8$, $N(CH_2CH_3)_3$), 3.21 (6H, s, NAr-2,6-$(CH_3)_2$), 1.38 (9H, t, $J=7.3$, $N(CH_2CH_3)_3$); ^{13}C, δ 169.61 ($-CO_2H\cdots NEt_3$), 161.29, 144.17, 133.33,

131.66, 130.80, 126.16, 125.86, 121.30, 121.05, 45.88 ($N(CH_2CH_3)_3$), 18.17 (NAr–2,6-$(CH_3)_2$), 8.78 ($N(CH_2CH_3)_3$). Analytical data for $C_{21}H_{29}N_2O_3WCl_3$. Calc.: 38.94% C, 4.51% H, 4.33% N. Found: 38.98% C, 4.43% H, 4.22% N.

4.22. *W(=NC$_6$H$_3$–2,6-Me$_2$)Cl$_3$(Hsal–5-Cl···NEt$_3$) (**6b**)*

This compound was prepared in a manner similar to **6a**, by combining **2b** (1.164 g, 2.00 mmol) in ~25 ml of dichloromethane and triethylamine (0.28 ml, 0.20 g, 1.97 mmol) in ~30 ml of hexane and stirring overnight. The product was obtained as rust-brown fine needles. Yield: 76% (as CH_2Cl_2 solvate, 1.175 g, 1.53 mmol). NMR ($CDCl_3$, 300 MHz): ^{1}H, δ 11.09 (H, bs, $-CO_2H\cdots NEt_3$), 8.15 (H, d, $J_{4-6}=2.7$, 6-H of Hsal–5-Cl), 7.46 (H, dd, $J_{3-4}=8.7$, 4-H of Hsal–5-Cl), 7.23 (2H, d, $J_o=7.7$, 3,5-H of imido), 6.87 (H, d, 3-H of Hsal–5-Cl), 6.61 (H, t, 4-H of NAr–2,6-$(CH_3)_2$), 5.30 (included CH_2Cl_2), 3.37 (6H, d of q, $-CH_2N\cdots HO_2C-$), 3.37 ($N(CH_2CH_3)_3$), 3.20 (6H, s, NAr–2,6-$(CH_3)_2$), 1.39 (9H, t, $J=7.3$, $N(CH_2CH_3)_3$); ^{13}C, δ 168.80 ($-CO_2H\cdots NEt_3$), 160.14, 144.50, 136.93, 133.41, 131.61, 131.31, 131.25, 126.47, 122.90, 122.80, 46.31 ($N(CH_2CH_3)_3$), 18.43 (NAr–2,6-$(CH_3)_2$), 9.11 ($N(CH_2CH_3)_3$).

4.23. *W(=NC$_6$H$_3$–2,6-Me$_2$)Cl$_3$(Hsal–3-Me···NEt$_3$) (**6c**)*

This dark red compound was prepared using **2c** (1.121 g, 2.00 mmol). Yield: 86.1% (1.140 g, 1.72 mmol). NMR ($CDCl_3$, 300 MHz): ^{1}H: δ 11.34 (1H, bs, $-CO_2H\cdots NEt_3$), 8.02 (1H, d), 7.42 (1H, d), 7.23 (2H, d), 7.01 (1H, t), 6.61 (1H, t), 3.37 (6H, m, $N(CH_2CH_3)_3$), 3.24 (6H, s, NAr–2,6-$(CH_3)_2$), 2.41 (3H, s, sal–3-CH_3), 1.38 (9H, t, $N(CH_2CH_3)_3$); ^{13}C, δ 169.96 ($-CO_2H\cdots NEt_3$), 160.20, 148.47, 142.71, 134.85, 130.24, 129.51, 126.15, 125.45, 121.19, 45.85 ($N(CH_2CH_3)_3$), 18.11 (NAr–2,6-$(CH_3)_2$), 16.97 (sal–3-CH_3), 8.76 ($N(CH_2CH_3)_3$). Analytical data for $C_{22}H_{31}N_2O_3WCl_3$. Calc.: 39.93% C; 4.72% H. Found: 39.81% C; 4.71% H.

4.24. *CH$_2$(C$_6$H$_4$–N=WCl$_4$···OEt$_2$)$_2$ (7)*

In a small Schlenk flask under nitrogen, $WOCl_4$ (5.125 g, 15.0 mmol) was slurried in 40 ml of toluene. To the mixture, 4,4′-methylene bis(phenylisocyanate) (1.877 g, 7.50 mmol) was added via an addition tube at ambient temperature. The magnetically stirred red mixture turned brown while refluxing for 2 h. After cooling to room temperature the solvent was removed in vacuo, then 30 ml of dichloromethane and 5 ml of diethyl ether were added and the solution mixture stirred over night. After removing the solvent in vacuo, 10 ml of diethyl ether and 40 ml of toluene were added and the slurry stirred briefly and filtered to afford the green product. Yield: 77% (5.77 g, 5.81 mmol). NMR data ($CDCl_3$, 300 MHz): ^{1}H, δ 7.53 (4H, d), 7.26 (4H, d), 5.08 (2H, s, CH_2 bridge), 4.63 (8H, m, $O(CH_2CH_3)_2$), 1.48 (12H, t, $O(CH_2CH_3)_2$); ^{13}C (partial), δ 148.26, 131.95, 127.71, 66.13 ($O(CH_2CH_3)_2$), 40.06 (CH_2 bridge), 13.28 ($O(CH_2CH_3)_2$).

4.25. $CH_2[C_6H_4{-}N{=}WCl_3(Hsal{-}3{-}Me{\cdots}OEt_2)]_2$ (**8b**)

This red compound was prepared in the same manner as **4c** using one equivalent of **7** and two equivalents of 3-methylsalicylic acid. Yield: 60% (0.74 g, 0.67 mmol). NMR data ($CDCl_3$, 300 MHz): ^1H, δ 14.64 (2H, bs, $-CO_2H{\cdots}OEt_2$), 8.06 (2H, d), 7.61 (2H, d), 7.43 (4H, d), 7.33 (4H, d), 7.12 (2H, t), 4.73 (2H, s, CH_2 bridge), 3.63 (8H, q, $O(CH_2CH_3)_2$), 2.40 (6H, s, sal–3-CH_3), 1.26 (12H, t, $O(CH_2CH_3)_2$).

4.26. $W(=O)Cl_2(sal{-}5{-}Cl)(THF)$ (**9b**)

In a small Schlenk flask under nitrogen, **1b** (0.54 g, 1.13 mmol) was dissolved in 20 ml of dry THF and stirred overnight at ambient temperature. Removing the solvent in vacuo yielded a dark purple crystalline material. Yield: 102% (0.59 g, 1.15 mmol). NMR ($CDCl_3$, 300 MHz): ^1H, δ 8.20 (1H, s), 7.74 (1H, d), 7.09 (1H, d), 4.05 (4H, t, OCH_2CH_2 of THF), 2.03 (4H, m, OCH_2CH_2 of THF); ^{13}C, δ 170.46 (carboxylate), 158.78, 136.40, 134.66, 131.60, 123.94, 120.10, 68.51 (OCH_2CH_2 of THF), 25.45 (OCH_2CH_2 of THF).

4.27. $W(=NC_6H_3{-}2,6{-}Me_2)Cl_2(sal{-}5{-}Cl)(THF)$ (**10b**)

This brown compound was prepared in a manner similar to **9b**. NMR ($CDCl_3$, 300 MHz): ^1H, δ 8.16 (1H, s), 7.63 (1H, d), 7.27 (2H, d), 6.98 (1H, d), 6.68 (1H, t), 4.03 (4H, t, OCH_2CH_2 of THF), 3.19 (6H, s, NAr–2,6-$(CH_3)_2$), 2.00 (4H, t, OCH_2CH_2 of THF); ^{13}C, δ 171.43 (carboxylate), 160.66, 149.00, 144.29, 136.77, 132.08, 131.23, 130.90, 126.36, 123.23, 117.64, 68.48 (OCH_2CH_2 of THF), 25.50 (OCH_2CH_2 of THF), 18.03 (NAr–2,6-$(CH_3)_2$).

4.28. Procedure for NMR titrations

The compound being titrated was weighed to the nearest hundredth of a milligram, dissolved in NMR solvent and diluted to the desired volume. This solution was either prepared in a calibrated NMR tube or transferred to a calibrated tube and diluted to the mark. The tube was capped with a rubber septum and the septum was secured with Parafilm®. The NMR solvent/ether titrant solution was prepared in a 1 ml class A volumetric flask. The [Et_2O] was either 2.86 M or 5.73 M, depending on the experiment and/or how many points were desired from the particular titration. Each 1 μl aliquot was injected via syringe, then the tube was inverted ten times to insure thorough mixing. The spectrum was acquired and the process repeated. The temperature of the NMR probe during the experiment was 20°C.

4.29. Structure determinations

Experimental parameters for the determination of the structures of **3e**, **4c**, and **6c** are listed in Table 8. All structures were solved by direct methods. Non-hydrogen atoms were refined anisotropically. All hydrogen atoms were placed at calculated

Table 8
Crystallographic data for solved structures

Compound	3e	4c	6c
Formula	$W_2Cl_6O_{10}C_{18}H_{20}$	$WCl_3N_1O_4C_{20}H_{26}$	$WCl_3N_2O_3C_{22}H_{31}$
Formula weight	976.77	634.64	661.71
Space group	$P2_1/n$ (#14)	$P\bar{1}$ (#2)	$C2/c$ (#15)
a (Å)	12.482(1)	8.435(1)	27.864(2)
b (Å)	15.478(2)	16.574(3)	14.174(1)
c (Å)	14.451(2)	8.240(1)	13.781(1)
α (deg)	90	91.45(2)	90
β (deg)	91.68(2)	94.59(2)	114.185(5)
γ (deg)	90	95.14(2)	90
V (Å^3)	2791(1)	1143.1(6)	4965(1)
Z	4	2	8
ρ(calc) (g cm^{-3})	2.325	1.844	1.770
Mo(Kα) (cm^{-1})	210.87	130.11	119.90
Temperature (K)	113	113	113
$R(F)$	0.055	0.048	0.036
$R_w(F)$	0.069	0.058	0.070

$$R=\frac{\Sigma\,||F_o|-|F_c||}{\Sigma\,|F_o|} \text{ and } R_w=\sqrt{\frac{\Sigma\,w(|F_o|-F_c|)^2}{\Sigma\,w|F_o|}}$$

positions, except for the triethylammonium proton of **6c**. Cromer and Waber's neutral atom scattering factors were used [45]. Anomalous dispersion effects were included in F_{calc}; the values employed for f' and f'' were Cromer's [46]. All calculations were performed using the TEXSAN crystallographic software package or MSC.

Acknowledgements

We acknowledge the Donors of the Petroleum Research Fund administered by the American Chemical Society for support of this research.

References

[1] T.A. Kabanos, A.D. Deramidas, A. Papaioannou, A. Terzis, Inorg. Chem. 33 (1994) 845.
[2] A. Houlton, D.M.P. Mingos, D.J. Williams, J. Chem. Soc. Chem. Commun. (1994) 503.
[3] B.L. Tsao, R.J. Pieters, J. Rebek, J. Am. Chem. Soc. 117 (1995) 2210.
[4] G. Pifat-Mrzljak (Ed.), Supramolecular Structure and Function, World Scientific, Singapore, 1988.
[5] P. Friedrich, Supramolecular Enzyme Organization, Pergamon Press, Oxford, UK, 1984.
[6] L.L. Kiefer, S.A. Paterno, C.A. Fierke, J. Am. Chem. Soc. 117 (1995) 6831.
[7] P.L. Alsters, P.J. Baesjou, M.D. Janssen, H. Kooijman, A. Sicherer-Roetman, A.L. Spek, G. van Koten, Organometallics 11 (1992) 4124.
[8] T.G. Richmond, Coord. Chem. Rev. 29 (1990) 221.
[9] J.P. Mathias, C.T. Seto, E.E. Simanek, G.M. Whitesides, J. Am. Chem. Soc. 116 (1994) 1725.
[10] A.D. Hamilton, M.S. Goodman, J. Weiss, J. Am. Chem. Soc. 117 (1995) 8447.

[11] T.G. Richmond, Coord. Chem. Rev. 105 (1990) 221.
[12] D. Braga, F. Grepioni, P. Sabatino, G.R. Desiraju, Organometallics 13 (1994) 3532.
[13] S. Subramanian, M.J. Zaworotko, Coord Chem. Rev. 137 (1994) 357.
[14] A. Lehtonen, R. Sillanpää, Polyhedron 14 (1995) 1831.
[15] T.A. Kabanos, A.D. Keramidas, A. Papaicannou, A. Terzis, Inorg. Chem. 33 (1994) 845.
[16] M.D. Morton, J.A. Heppert, S.D. Dietz, W.H. Huang, D.A. Ellis, T.A. Grant, N.W. Eilerts, D.L. Barnes, F. Takusagawa, D. VanderVelde, J. Am. Chem. Soc. 115 (1993) 7916.
[17] T.E. Baroni, J.A. Heppert, R.R. Hodel, R.P. Kingsborough, M.D. Morton, A.L. Rheingold, G.P.A. Yap, Organometallics 15 (1996) 4872 and references cited therein
[18] C. Person, A. Oskarsson, C. Andersson, Polyhedron 16 (1992) 2039.
[19] A. Bell, J. Mol. Catal. 76 (1991) 165.
[20] C.F. Edwards, W.P. Griffith, H.A.P. White, D.J. Williams, Polyhedron 11 (1992) 2711.
[21] H. Funk, G.Z. Mohaupt, Anorg. Allg. Chem. B 315 (1962) 204.
[22] W.P. Griffith, H.I.S. Nogueria, B.C. Parkin, R.N. Sheppard, A.J.P. White, D.J. Williams, J. Chem. Soc. Dalton Trans. (1995) 1775.
[23] W.P. Griffith, C.F. Edwards, A.J.P. White, D.J. Williams, J. Chem. Soc. Dalton Trans. (1993) 3813.
[24] A. Lehtonen, R. Sillanpää, J. Chem. Soc. Dalton Trans. (1994) 2119.
[25] L.K. Johnson, S.C. Virgil, R.H. Grubbs, J. Am. Chem. Soc. 112 (1990) 5384.
[26] K.H. Theopold, S.J. Holmes, R.R. Schrock, Angew. Chem. Int. Ed. Engl. 22 (1983) 1010.
[27] E.P. Clark, Ind. Eng. Chem. Anal. Ed. 13 (1941) 820.
[28] C.B. Aakeröy, K.R. Seddon, Chem. Soc. Rev. (1993) 397.
[29] W.C. Hamilton, Hydrogen Bonding in Solids, W.A. Benjamin, New York, 1968.
[30] P.J. Davies, N. Veldman, D.M. Grove, A.L. Spek, B.T.G. Lutz, G. van Koten, Angew. Chem. Int. Ed. Engl. 35 (1996) 1959.
[31] G.P.A. Yap, A.L. Rheingold, P. Das, R.H. Crabtree, Inorg. Chem. 34 (1995) 3474.
[32] N.B. Chapman, J. Shorter (Eds.), Correlation Analysis in Chemistry, Plenum Press, New York, 1978, pp. 357–396.
[33] L.P. Hammett, Physical Organic Chemistry, McGraw Hill, New York, 1970.
[34] C.J. Giffney, C.J. O'Connor, J. Magn. Reson. 18 (1975) 230.
[35] P. Gilli, V. Bertolasi, V. Ferretti, G. Gilli, J. Am. Chem. Soc. 116 (1994) 909.
[36] H.-B. Bürgi, J.D. Dunnitz (Eds.), Structure Correlation, VCH, New York, 1994, pp. 523–529.
[37] G.R. Desiraju, A. Gavezzotti, Acta Crystallogr. Sect. B: 45 (1989) 473.
[38] T. Kawamoto, B.S. Hammes, B. Haggerty, G.P.A. Yap, A.L. Rheingold, A.S. Borovik, J. Am. Chem. Soc. 118 (1996) 285.
[39] T.B. Karpishin, T.D.P. Stack, K.N. Raymond, J. Am. Chem. Soc. 115 (1993) 6115.
[40] S.K. Burley, G.A. Petsko, Science 229 (1985) 23.
[41] C.A. Hunter, Chem. Soc. Rev. (1994) 101.
[42] D.E. Wigley, in: K.D. Karlin (Ed.), Progress in Inorganic Chemistry, vol. 42, Wiley, p. 239.
[43] W.A. Nugent, J.M. Mayer, Metal Ligand Multiple Bonds, Wiley Interscience, New York, 1988, p. 183.
[44] R.D. Green, Hydrogen Bonding by C–H Groups, Halsted Press, New York, 1974, pp. 26–30.
[45] D.T., Cromer, J.T. Waber, International Tables for X-Ray Crystallography, vol. 4, Kynoch Press, Birmingham, UK, 1974, Table 2.2A.
[46] D.T. Cromer, International Tables for X-Ray Crystallography, vol. 4, Kynoch Press, Birmingham, UK, 1974, Table 2.3.1.